

Can we distinguish black holes with electric and magnetic charges from quasinormal modes?

Antonio De Felice¹ and Shinji Tsujikawa²

¹*Center for Gravitational Physics and Quantum Information,*

Yukawa Institute for Theoretical Physics, Kyoto University, 606-8502, Kyoto, Japan

²*Department of Physics, Waseda University, 3-4-1 Okubo, Shinjuku, Tokyo 169-8555, Japan*

(Dated: December 7, 2023)

We compute the quasinormal modes of static and spherically symmetric black holes (BHs) with electric and magnetic charges. For the electrically charged case, the dynamics of perturbations separates into the odd- and even-parity sectors with two coupled differential equations in each sector. In the presence of both electric and magnetic charges, the differential equations of four dynamical degrees of freedom are coupled with each other between odd- and even-parity perturbations. Despite this notable modification, we show that, for a given total charge and mass, a BH with mixed electric and magnetic charges gives rise to the same quasinormal frequencies for fundamental modes. This includes the case in which two BHs have equal electric and magnetic charges for each of them. Thus, the gravitational-wave observations of quasinormal modes during the ringdown phase alone do not distinguish between electrically and magnetically charged BHs.

I. INTRODUCTION

General Relativity (GR) is a fundamental pillar for describing the gravitational interaction in curved spacetime [1]. The Schwarzschild black hole (BH) [2], which is characterized by a mass M , corresponds to a vacuum solution in GR on a static and spherically symmetric (SSS) background. If we take an electromagnetic field into account, the SSS BH solution is given by a Reissner-Nordström (RN) metric [3, 4] containing an electric charge q_E besides the BH mass M . The Einstein field equations of motion also admit the existence of BHs with a magnetic charge q_M .

Unlike the electrically charged case, the magnetically charged BH is not neutralized with ordinary matter in conductive media. Hence the latter can be a long-lived stable configuration which is interpreted as a kind of magnetic monopole [5, 6]. Moreover, the presence of primordial BHs in the early Universe could absorb magnetic monopoles [7–11]. Since the BH magnetic charge generates large magnetic fields in the vicinity of the horizon [5, 12, 13], the signature of such field configurations can be probed from observations. To distinguish between electrically and magnetically charged BHs, it is important to understand their basic theoretical properties and confront them with observations.

From the observational side, the BH shadows probed by the Event Horizon Telescope (EHT) [14] started to put constraints on the total charges of BHs [15]. This analysis includes not only charged BHs in GR but also those arising in string theory such as the Maxwell-dilaton BH [16–18] and the Sen BH [19]. These solutions generally contain both the electric and magnetic charges in the background metric components. The electromagnetic and gravitational radiations emitted from charged binary BHs modify the merger time [20–22] as well as the phase of gravitational waveforms [23]. The electric dipole radiation [24, 25] should be similar to the scalar dipole radiation in scalar-tensor theory, in that the leading-order modification to the phase appears as the -1 post-Newtonian order [26–30]. The analysis with the BH-neutron star merger events GW200105 and GW200115 put an upper bound on the BH electric charge [31] (see also Ref. [32]). Note that this is analogous to constraints on the scalar charge of neutron stars recently analyzed with the GW200115 signal [33, 34] (see also Ref. [35]).

After the merging of compact binaries, there is a ringdown phase in which the emission of gravitational waves is characterized by a spectrum of particular frequencies and damping proper oscillations. This signal is dominated by a so-called quasinormal mode (QNM) with the lowest frequency. Since the QNMs are different depending on to what extent the BHs have hairs, it is possible to observationally distinguish between different BH solutions (see Refs. [36–40] for reviews). Although the current gravitational wave observations have not precisely measured the tensor waveform in the ringdown phase, the next-generation detectors will offer a possibility for probing the physics in strong gravity regimes through the quasinormal frequencies.

The QNMs of BHs can be computed by exploiting the gravitational perturbation theory originally developed by Regge and Wheeler [41] and Zerilli [42, 43]. The perturbations on a SSS background can be decomposed into odd- and even-parity modes according to the transformation properties under a two-dimensional rotation of the sphere. In spite of the difference in potentials between the odd- and even-parity perturbations, Chandrasekhar and Detweiler [44] showed that the QNMs of the Schwarzschild BH are the same for both parities. This isospectrality can be understood by the presence of a single superpotential generating the potentials in both odd- and even-parity sectors [45, 46].

For the RN BH with an electric charge q_E , the perturbation equations of motion, which were originally derived by Moncrief [47–49] and Zerilli [50], separate into the odd- and even-parity modes. In each parity sector, there are

two dynamical degrees of freedom arising from the gravitational and electromagnetic perturbations coupled with each other. Since the solutions of even-parity perturbations can be deduced from those of odd-parity modes [51], it is sufficient to compute the QNMs of gravitational and electromagnetic perturbations in the odd-parity sector. In other words, the QNMs of electrically charged BHs can be found by integrating two coupled differential equations of odd-parity perturbations. The boundary conditions of QNMs correspond to those of purely ingoing waves at the horizon and purely outgoing at spatial infinity.

Following the numerical method of Chandrasekhar and Detweiler [44], the QNMs of electrically charged RN BHs were originally computed by Gunter [52]. Kokkotas and Schutz [53] calculated the QNMs by exploiting a high-order WKB approximation advocated in Refs. [54, 55] and showed that the WKB method reproduces the numerical results within 1% accuracy for fundamental modes. For the potentials containing only the powers of $1/r$, it is known that a continued-fraction representation of wave functions [56, 57] is the most accurate and efficient method for the computation of QNMs [40]. Indeed, Leaver applied this continued-fraction method to the calculation of QNMs for electrically charged RN BHs [58] (see also Refs. [59]). This analysis was further extended to the (nearly) extreme RN BHs [60, 61].

For a magnetically charged BH, the perturbation equations of motion were derived in Ref. [62] in generalized Einstein-Maxwell theories containing nonlinear functions of the electromagnetic field strength. Reflecting the different properties of parities for the magnetic charge q_M compared to the electric charge q_E , the system of linear perturbations separates into the two types: (I) the odd-parity gravitational and even-parity electromagnetic perturbations are coupled, which we call type I, and (II) the even-parity gravitational and odd-parity electromagnetic perturbations are coupled, which we call type II. In Ref. [63], it was shown that the isospectrality of QNMs between types (I) and (II) holds in standard Einstein-Maxwell theory, while it is broken by the nonlinear electromagnetic field strength. This means that the QNMs of magnetic BHs in standard Einstein-Maxwell theory can be known by solving the two coupled differential equations either for type (I) or (II).

While the past works of QNMs focused on either the purely electric or magnetic BH (for which the pseudoscalar $F_{\mu\nu}\tilde{F}^{\mu\nu}$ vanishes on the SSS background), it is not yet clear whether the coexistence of two different charges gives rise to a new feature for the QNM spectrum. In this paper, we will compute the QNMs of BHs with mixed electric and magnetic charges in standard Einstein-Maxwell theory. For this more general configuration, the background value of the pseudo-scalar $F_{\mu\nu}\tilde{F}^{\mu\nu}$ does not vanish. To the best of our knowledge, the same analysis was not performed elsewhere. We will show that, for $q_M \neq 0$ and $q_E \neq 0$, the odd- and even-parity perturbation equations of four dynamical degrees of freedom (two gravitational and two electromagnetic) are coupled with each other. Thus, the computation of QNMs is more involved in comparison to purely electric or magnetic BHs.

Upon using matrix-valued direct integration methods (see e.g., Ref. [40]), we will show that, for a given total BH charge $\sqrt{q_E^2 + q_M^2}$ and mass M , the QNMs with a fixed multipole moment l are the same independent of the ratio between the electric and magnetic charges. This property is far from trivial due to the very different structure of the coupled differential equations of four dynamical perturbations. As a special case, we confirm the property that two BHs with purely electric and magnetic charges also have the equivalent QNMs. Thus, the gravitational waveforms during the ringdown phase alone do not generally distinguish between the two different BH charges.

This paper is organized as follows. In Sec. II, we revisit the BH solution in the presence of both electric and magnetic charges. In Sec. III, we will obtain the total second-order action containing both odd- and even-parity perturbations and derive the coupled differential equations of four dynamical degrees of freedom. In Sec. IV, we will explain the matrix-valued direct integration method for the computation of QNMs in our Einstein-Maxwell theory. In Sec. V, we will present our numerical results and show that, independent of the ratio between electric and magnetic charges, the QNMs are determined by the total BH charge and mass. Sec. VI is devoted to conclusions.

II. CHARGED BLACK HOLES

We begin with Einstein-Maxwell theories given by the action

$$\mathcal{S} = \int d^4x \sqrt{-g} \left(\frac{M_{\text{Pl}}^2}{2} R - \frac{1}{4} F_{\mu\nu} F^{\mu\nu} \right), \quad (2.1)$$

where M_{Pl} is the reduced Planck mass, g is a determinant of the metric tensor $g_{\mu\nu}$, R is the Ricci scalar, and $F_{\mu\nu} = \partial_\mu A_\nu - \partial_\nu A_\mu$ is the electromagnetic field strength with a vector field A_μ . The action (2.1) respects the $U(1)$ gauge symmetry under the shift $A_\mu \rightarrow A_\mu + \partial_\mu \chi$.

We study the QNMs of charged BHs on a SSS background given by the line element

$$ds^2 = -f(r)dt^2 + h^{-1}(r)dr^2 + r^2 (d\theta^2 + \sin^2 \theta d\varphi^2), \quad (2.2)$$

where t , r and (θ, φ) represent the time, radial, and angular coordinates (in the ranges $0 \leq \theta < \pi$ and $0 \leq \varphi < 2\pi$), respectively, and f and h are functions of r . For the vector field, we consider the following configuration

$$A_\mu = [A_0(r), 0, 0, A_\varphi(\theta)], \quad (2.3)$$

where A_0 and A_φ depend on r and θ , respectively.

On the background (2.2), the scalar product $F_{\mu\nu}F^{\mu\nu}/4$ is expressed as

$$\frac{1}{4}F_{\mu\nu}F^{\mu\nu} = \frac{1}{2r^4} \left(\frac{dA_\varphi}{dz} \right)^2 - \frac{h}{2f} (A'_0)^2, \quad (2.4)$$

where $z = \cos \theta$, and a prime here and in the following denotes the differentiation with respect to r . For the compatibility with spherical symmetry, we require that $A_\varphi \propto z$ (up to an irrelevant constant). Then, we will choose

$$A_\varphi = -q_M z = -q_M \cos \theta, \quad (2.5)$$

where q_M is a constant corresponding to the magnetic charge. Now, the vector-field configuration is given by

$$A_\mu dx^\mu = A_0(r) dt - q_M \cos \theta d\varphi. \quad (2.6)$$

Varying the action (2.1) with respect to $g_{\mu\nu}$ and A_μ , we obtain the following gravitational and vector-field equations of motion

$$M_{\text{Pl}}^2 r h' + M_{\text{Pl}}^2 (h - 1) + \frac{q_M^2}{2r^2} + \frac{(A'_0)^2 r^2 h}{2f} = 0, \quad (2.7)$$

$$M_{\text{Pl}}^2 r f' + M_{\text{Pl}}^2 \frac{f(h-1)}{h} + \frac{q_M^2 f}{2r^2 h} + \frac{A_0'^2 r}{2} = 0, \quad (2.8)$$

$$A_0'' + \left(\frac{2}{r} - \frac{f'}{2f} + \frac{h'}{2h} \right) A_0' = 0, \quad (2.9)$$

where a prime represents the derivative with respect to r . The solution to Eq. (2.9) is given by

$$A_0'(r) = \frac{\sqrt{f} q_E}{r^2 \sqrt{h}}, \quad (2.10)$$

where the integration constant q_E corresponds to the electric charge. Substituting Eq. (2.10) into Eqs. (2.7) and (2.8) and imposing the asymptotically flat boundary conditions $f(\infty) = h(\infty) = 1$, we obtain the following integrated solutions

$$f(r) = h(r) = 1 - \frac{2M}{r} + \frac{q_E^2 + q_M^2}{2M_{\text{Pl}}^2 r^2}, \quad (2.11)$$

where M is an integration constant corresponding to the BH mass. Thus, the squared total BH charge is given by

$$q_T^2 = q_E^2 + q_M^2. \quad (2.12)$$

So long as the background metric is concerned, the magnetic charge q_M is not distinguished from the electric charge q_E . We are interested in whether the mixture of electric and magnetic charges affects the QNMs of BHs. For this purpose, we need to formulate the BH linear perturbation theory on the SSS background (2.2).

III. BLACK HOLE PERTURBATIONS

Let us consider metric perturbations $h_{\mu\nu}$ on the background (2.2). They can be decomposed into odd- and even-parity modes depending on the parity transformation under a rotation in the (θ, φ) plane [41–43]. We expand all the perturbations in terms of the spherical harmonics $Y_{lm}(\theta, \varphi)$. We can set $m = 0$ with the loss of generality, in which case Y_{l0} is a function of $z = \cos \theta$. The odd modes have the parity $(-1)^{l+1}$, whereas the even modes possess the parity $(-1)^l$.

The tt , tr , and rr components of $h_{\mu\nu}$ contain only the even-parity perturbations as

$$h_{tt} = f(r) \sum_l H_0(t, r) Y_{l0}(\theta), \quad h_{tr} = h_{rt} = \sum_l H_1(t, r) Y_{l0}(\theta), \quad h_{rr} = h(r)^{-1} \sum_l H_2(t, r) Y_{l0}(\theta), \quad (3.1)$$

where H_0 , H_1 , and H_2 are functions of t and r . The perturbations h_{ab} , where a and b represent either θ or φ , can be expressed in the form

$$h_{ab} = \frac{1}{2} \sum_l U(t, r) [(E_a)^c \nabla_c \nabla_b Y_{l0}(\theta) + (E_b)^c \nabla_c \nabla_a Y_{l0}(\theta)] + \sum_l [K(t, r) g_{ab} Y_{l0}(\theta) + G(t, r) \nabla_a \nabla_b Y_{l0}(\theta)], \quad (3.2)$$

where ∇_a is the 2-dimensional covariant derivative operator, and E_{ab} is an anti-symmetric tensor with the nonvanishing components $E_{\varphi\theta} = -E_{\theta\varphi} = -\sin\theta$. The quantity U is associated with the odd-parity perturbation, whereas K and G correspond to the even-parity perturbations. In the following, we will choose the gauge

$$U(t, r) = 0, \quad K(t, r) = 0 = G(t, r), \quad (3.3)$$

under which all the components of h_{ab} vanish. The ta and ra components of $h_{\mu\nu}$ can be expressed as

$$h_{ta} = h_{at} = \sum_l h_0(t, r) \nabla_a Y_{l0}(\theta) + \sum_l Q(t, r) E_{ab} \nabla^b Y_{l0}(\theta), \quad (3.4)$$

$$h_{ra} = h_{ar} = \sum_l h_1(t, r) \nabla_a Y_{l0}(\theta) + \sum_l W(t, r) E_{ab} \nabla^b Y_{l0}(\theta), \quad (3.5)$$

where h_0 and h_1 correspond to the even-parity perturbations, and Q and W are the perturbations in the odd-parity sector. We choose the gauge

$$h_0(t, r) = 0. \quad (3.6)$$

All of the residual gauge degrees of freedom are fixed under the gauge choices (3.3) and (3.6). Then, the nonvanishing metric components are

$$\begin{aligned} g_{tt} &= -f(r) + f(r) \sum_l H_0(t, r) Y_{l0}(\theta), & g_{tr} &= g_{rt} = \sum_l H_1(t, r) Y_{l0}(\theta), & g_{t\varphi} &= g_{\varphi t} = -\sum_l Q(t, r) (\sin\theta) Y_{l0,\theta}(\theta), \\ g_{rr} &= h^{-1}(r) + h^{-1}(r) \sum_l H_2(t, r) Y_{l0}(\theta), & g_{r\theta} &= g_{\theta r} = \sum_l h_1(t, r) Y_{l0,\theta}(\theta), \\ g_{r\varphi} &= g_{\varphi r} = -\sum_l W(t, r) (\sin\theta) Y_{l0,\theta}(\theta), & g_{\theta\theta} &= r^2, & g_{\varphi\varphi} &= r^2 \sin^2\theta, \end{aligned} \quad (3.7)$$

where $Y_{l0,\theta} \equiv dY_{l0}/d\theta$.

The vector field A_μ has a perturbed component $\delta A_\varphi = \sum_l \delta A(t, r) E_{\varphi\theta} \nabla^\theta Y_{l0}(\theta)$ in the odd-parity sector, where δA is a function of t and r . In the even-parity sector, the existence of a $U(1)$ gauge symmetry allows us to choose the gauge $A_\theta = 0$ [64]. Then, the components of A_μ can be expressed as

$$\begin{aligned} A_t &= A_0(r) + \sum_l \delta A_0(t, r) Y_{l0}(\theta), & A_r &= \sum_l \delta A_1(t, r) Y_{l0}(\theta), & A_\theta &= 0, \\ A_\varphi &= -q_M \cos\theta - \sum_l \delta A(t, r) (\sin\theta) Y_{l0,\theta}(\theta), \end{aligned} \quad (3.8)$$

where δA_0 and δA_1 are functions of t and r in the even-parity sector.

We expand the action (2.1) up to second order in perturbations and integrate the quadratic-order action with respect to θ . We drop the boundary terms after the integration by parts with respect to r . In the second-order action, the multipole moments appear as the combination

$$L \equiv l(l+1). \quad (3.9)$$

Since the tensor gravitational waves are not generated from the monopole ($l=0$) and dipole ($l=1$) modes, we will focus on the case

$$l \geq 2, \quad (3.10)$$

in the following.

On using the property $f = h$ for the background BH solution (2.11), the second-order action of perturbations can be expressed in the form $\mathcal{S}^{(2)} = \int dt dr \mathcal{L}$, where

$$\mathcal{L} = \mathcal{L}_A + \mathcal{L}_B, \quad (3.11)$$

with

$$\begin{aligned} \mathcal{L}_A = & \frac{LM_{\text{Pl}}^2}{4} \left(\dot{W} - Q' + \frac{2Q}{r} \right)^2 - \frac{Lq_E}{r^2} \left(\dot{W} - Q' + \frac{2Q}{r} \right) \delta A + \frac{L[M_{\text{Pl}}^2(L-2)r^2 + 2q_M^2]}{4r^4 f} (Q^2 - f^2 W^2) \\ & + \frac{L}{2f} \left(\delta \dot{A}^2 - f^2 \delta A'^2 - \frac{fL}{r^2} \delta A^2 \right) - \frac{Lq_E q_M}{r^4} Q h_1 + \frac{Lq_M}{r^2 f} (Q \delta A_0 - f^2 W \delta A_1) \\ & - \frac{Lq_M}{2r^2} [2f \delta A' h_1 - \delta A (H_0 - H_2)], \end{aligned} \quad (3.12)$$

and

$$\begin{aligned} \mathcal{L}_B = & \frac{q_E^2}{8r^2} H_0^2 - \left[\frac{rM_{\text{Pl}}^2 f}{2} H_2' - \frac{LM_{\text{Pl}}^2 f}{2} h_1' + \frac{M_{\text{Pl}}^2(L+2)r^2 - q_M^2}{4r^2} H_2 - L \frac{2M_{\text{Pl}}^2 r^2 (f+1) - q_E^2 - q_M^2}{8r^3} h_1 \right] H_0 \\ & + \frac{LM_{\text{Pl}}^2}{4} H_1^2 + M_{\text{Pl}}^2 \left(r \dot{H}_2 - \frac{L}{2} \dot{h}_1 \right) H_1 + \frac{2M_{\text{Pl}}^2 r^2 - q_M^2}{8r^2} H_2^2 - L \frac{2M_{\text{Pl}}^2 r^2 (f+1) - q_E^2 - q_M^2}{8r^3} H_2 h_1 \\ & + \frac{LM_{\text{Pl}}^2}{4} \dot{h}_1^2 + \frac{Lf(M_{\text{Pl}}^2 r^2 - q_M^2)}{2r^4} h_1^2 + \frac{r^2}{2} (\delta A_0' - \delta \dot{A}_1)^2 + \frac{q_E}{2} (H_0 - H_2) (\delta A_0' - \delta \dot{A}_1) \\ & - L \left(\frac{q_E}{r^2} h_1 \delta A_0 - \frac{1}{2f} \delta A_0^2 + \frac{f}{2} \delta A_1^2 \right). \end{aligned} \quad (3.13)$$

Here, a dot represents the derivative with respect to t . The total Lagrangian density \mathcal{L} contains the nine perturbations $Q, W, H_0, H_1, H_2, h_1, \delta A_0, \delta A_1$, and δA . In the following, we will show that this system is described by four dynamical perturbations after integrating out all the nondynamical fields. First of all, we introduce a Lagrangian multiplier χ_1 as follows

$$\mathcal{L}_2 = \mathcal{L} - \frac{LM_{\text{Pl}}^2}{4} \left(\dot{W} - Q' + \frac{2Q}{r} - \frac{2q_E}{M_{\text{Pl}}^2 r^2} \delta A - \chi_1 \right)^2. \quad (3.14)$$

Varying \mathcal{L}_2 with respect to χ_1 , it follows that

$$\chi_1 = \dot{W} - Q' + \frac{2Q}{r} - \frac{2q_E}{M_{\text{Pl}}^2 r^2} \delta A. \quad (3.15)$$

Substituting Eq. (3.15) into Eq. (3.14), we find that \mathcal{L}_2 is equivalent to \mathcal{L} . By introducing χ_1 , the Lagrangian \mathcal{L}_2 does not contain the derivative terms like \dot{W}^2 , $(Q')^2$, and $\delta A Q'$. Varying \mathcal{L}_2 with respect to Q and W , we obtain

$$Q = - \frac{M_{\text{Pl}}^2 r^3 f (r \chi_1' + 2\chi_1) + 2q_M (r^2 \delta A_0 - q_E f h_1)}{M_{\text{Pl}}^2 (L-2)r^2 + 2q_M^2}, \quad (3.16)$$

$$W = - \frac{r^2 [M_{\text{Pl}}^2 r^2 \dot{\chi}_1 + 2q_M f \delta A_1]}{[M_{\text{Pl}}^2 (L-2)r^2 + 2q_M^2] f}. \quad (3.17)$$

We use these relations to eliminate Q, W and their derivatives from the action. After this procedure, we find that the action contains the two dynamical perturbations χ_1 and δA arising from the odd-parity sector.

The next procedure is to eliminate nondynamical perturbations in the even-parity sector. First of all, the equation of motion for H_1 is given by

$$H_1 = \dot{h}_1 - \frac{2r}{L} \dot{H}_2, \quad (3.18)$$

which is used to eliminate H_1 . As the next step, we study the equation of motion for H_0 . In order to express the r -derivative terms with respect to one single field, it is convenient to remove H_2 by means of the following field redefinition

$$v_1 = H_2 - \frac{L}{r} h_1. \quad (3.19)$$

At this point, we introduce for the Lagrangian density \mathcal{L}_2 a new Lagrange multiplier χ_2 as follows

$$\mathcal{L}_3 = \mathcal{L}_2 - \frac{r^2}{2} \left[\delta \dot{A}_1 - \delta A'_0 - \frac{q_E(H_0 - v_1)}{2r^2} + \frac{Lq_E h_1}{2r^3} - \chi_2 \right]^2, \quad (3.20)$$

whose variation with respect to χ_2 leads to

$$\chi_2 = \delta \dot{A}_1 - \delta A'_0 - \frac{q_E(H_0 - v_1)}{2r^2} + \frac{Lq_E h_1}{2r^3}. \quad (3.21)$$

Substituting Eq. (3.21) into Eq. (3.20), it follows that \mathcal{L}_3 is equivalent to \mathcal{L}_2 . The Lagrange multiplier χ_2 has been introduced for several purposes. First of all, we have now removed the H_0^2 term (as well as the couplings between H_0 and $\delta \dot{A}_1$ and $\delta A'_0$), so that the simplified equation of motion for H_0 can be used to integrate out h_1 in terms of the other variables as follows

$$\left[r^2(L - 3f + 1)M_{\text{Pl}}^2 - \frac{q_E^2}{2} - \frac{q_M^2}{2} \right] \frac{L}{r} h_1 = 2q_M L \delta A - 2M_{\text{Pl}}^2 r^3 f v'_1 - [M_{\text{Pl}}^2(L + 2)r^2 - q_E^2 - q_M^2] v_1 - 2q_E r^2 \chi_2. \quad (3.22)$$

The second purpose of this step is to remove the terms in $\delta \dot{A}_1^2$ and $(\delta A'_0)^2$ from the Lagrangian density, so that the fields δA_0 and δA_1 can be integrated out. In fact, the couplings in Eq. (3.20) between χ_2 and v_1 as well as χ_2 and h_1 have been introduced to simplify the equations of motion for δA_0 and δA_1 . Indeed, the equation of motion for δA_1 is given by

$$\delta A_1 = \frac{q_M}{f(L - 2)} \dot{\chi}_1 - \frac{M_{\text{Pl}}^2(L - 2)r^2 + 2q_M^2}{M_{\text{Pl}}^2 f L(L - 2)} \dot{\chi}_2. \quad (3.23)$$

Eliminating the fields δA_0 and δA_1 from the Lagrangian density \mathcal{L}_3 , we are left with the four dynamical perturbations δA , χ_1 , χ_2 , and v_1 . After a few integrations by parts, we obtain the reduced Lagrangian in the form

$$\mathcal{L}_F = \vec{\Psi}^T \mathbf{K} \dot{\vec{\Psi}} + \vec{\Psi}'^T \mathbf{G} \vec{\Psi}' + \vec{\Psi}^T \mathbf{M} \vec{\Psi} + \vec{\Psi}'^T \mathbf{Q} \vec{\Psi}, \quad (3.24)$$

where

$$\vec{\Psi} = (\delta A, \chi_1, \chi_2, v_1)^T. \quad (3.25)$$

Note that \mathbf{K} , \mathbf{G} , \mathbf{M} are 4×4 symmetric matrices, whereas \mathbf{Q} is a 4×4 anti-symmetric matrix. Out of the Lagrangian (3.24), we can easily derive conditions for the absence of ghosts. This requires that the determinants of principal submatrices of \mathbf{K} are positive, i.e.,

$$\begin{aligned} K_{11} &= \frac{L}{2f} > 0, & K_{11}K_{22} - K_{12}^2 &= \frac{M_{\text{Pl}}^2 L^2 r^2}{8f^2(L - 2)} > 0, & \det \mathbf{K}_3 &= \frac{M_{\text{Pl}}^2 L r^6}{16f^3(L - 2)} > 0, \\ \det \mathbf{K} &= \frac{M_{\text{Pl}}^8 r^{12}}{4f^2[2M_{\text{Pl}}^2(L + 1)r^2 - 6M_{\text{Pl}}^2 r^2 f - q_E^2 - q_M^2]^2} > 0, \end{aligned} \quad (3.26)$$

where \mathbf{K}_3 is the 3×3 matrix composed by the components without the 4-th subscript. For $l \geq 2$, all these four no-ghost conditions are trivially satisfied outside the horizon.

We vary the Lagrangian (3.24) with respect to δA , χ_1 , χ_2 , v_1 and solve their perturbation equations of motion for $\delta \ddot{A}$, $\ddot{\chi}_1$, $\ddot{\chi}_2$, \ddot{v}_1 . They are given, respectively, by

$$\begin{aligned} \delta \ddot{A} &= f^2 \delta A'' - \frac{f(L - \beta + f)}{r} \delta A' - \frac{f[(5L - 4\beta + 4)(3f - \beta)M_{\text{Pl}}^2 r^2 - 2q_M^2(5f - \beta)]}{M_{\text{Pl}}^2(3f - \beta)r^4} \delta A \\ &\quad - \frac{2f^2 q_M [2M_{\text{Pl}}^2 r f v'_1 + M_{\text{Pl}}^2(2\beta - L)v_1 + 2q_E \chi_2]}{M_{\text{Pl}}^2 L(3f - \beta)r^2} - \frac{f q_E}{r^2} \chi_1, \\ \ddot{\chi}_1 &= f^2 \chi_1'' - \frac{f(L - \beta - f)}{r} \chi_1' - \frac{f[M_{\text{Pl}}^2(3L + 4f - 2\beta - 2)r^2 + 2q_M^2]}{M_{\text{Pl}}^2 r^4} \chi_1 + \frac{4q_M f^2}{M_{\text{Pl}}^2 L r} \chi_2' \\ &\quad + \frac{2q_M f \{ (5f + \beta)L + 4f(3f - 3\beta + 2) \} M_{\text{Pl}}^2 r^2 - 4f q_M^2}{M_{\text{Pl}}^4 L(3f - \beta)r^4} \chi_2 + \frac{4q_E q_M f^2 [2r f v'_1 + (2\beta - L)v_1]}{M_{\text{Pl}}^2 L(3f - \beta)r^4} \end{aligned} \quad (3.27)$$

$$-\frac{2q_E f[(L-2)(3f-\beta)M_{\text{P}1}^2 r^2 + 2q_M^2(5f-\beta)]}{M_{\text{P}1}^4(3f-\beta)r^6} \delta A, \quad (3.28)$$

$$\begin{aligned} \ddot{\chi}_2 = & f^2 \chi_2'' - \frac{f(L-\beta-3f)}{r} \chi_2' - \frac{f[M_{\text{P}1}^2\{(L+2\beta-8)f-3\beta L+2\beta^2\}r^2 + 4fq_M^2]}{M_{\text{P}1}^2(3f-\beta)r^4} \chi_2 \\ & - \frac{q_M f L}{r^4} \chi_1 + \frac{2q_E f[2M_{\text{P}1}^2 r^3 f^2 v_1' - M_{\text{P}1}^2(L-2\beta)r^2 f v_1 - Lq_M(5f-\beta)\delta A]}{M_{\text{P}1}^2(3f-\beta)r^6}, \end{aligned} \quad (3.29)$$

$$\begin{aligned} \ddot{v}_1 = & f^2 v_1'' + \frac{f[(L+4)f+3f^2+3\beta(L-\beta)]}{(3f-\beta)r} v_1' + \frac{3(L-\beta+2)f^2 + f[(7L+2)\beta-4\beta^2-2L^2-2L] - \beta(L-\beta)^2}{(3f-\beta)r^2} v_1 \\ & - \frac{2\beta L + 4fL - \beta^2 - 4f\beta - 3f^2 + 4f}{M_{\text{P}1}^2(3f-\beta)r^4} (Lq_M \delta A - q_E r^2 \chi_2), \end{aligned} \quad (3.30)$$

where

$$\beta \equiv \frac{2M_{\text{P}1}^2(L+1)r^2 - q_E^2 - q_M^2}{2M_{\text{P}1}^2 r^2}. \quad (3.31)$$

We assume the solutions to the perturbation equations in the form $\vec{\Psi} \propto \vec{\Psi}_0 e^{-i(\omega t - kr)}$, where $\vec{\Psi}_0$ is a constant vector, ω and k are the angular frequency and wavenumber, respectively. In the limits of large ω and k , the dispersion relation corresponding to the radial propagation is given by

$$\det |f^2 c_r^2 \mathbf{K} + \mathbf{G}| = 0, \quad (3.32)$$

where c_r is the radial propagation speed measured by a rescaled radial coordinate $\tilde{r} = \int dr/\sqrt{f}$ and a proper time $\tau = \int dt \sqrt{f}$, such that $c_r = d\tilde{r}/d\tau$. Substituting the components of \mathbf{K} and \mathbf{G} into Eq. (3.32), it follows that

$$(c_r^2 - 1)^4 f^8 \det \mathbf{K} = 0. \quad (3.33)$$

Then, we obtain the following four solutions

$$c_r^2 = 1. \quad (3.34)$$

This means that all four dynamical perturbations δA , χ_1 , χ_2 , and v_1 have luminal propagation speeds.

To obtain the angular propagation speeds, we assume the solutions in the form $\vec{\Psi} = \vec{\Psi}_0 e^{-i\omega t}$. In the limits of large ω and l , the matrix components in \mathbf{G} and \mathbf{Q} do not contribute to the dispersion relation and hence

$$\det |fL c_\Omega^2 \mathbf{K} + r^2 \mathbf{M}| = 0, \quad (3.35)$$

where $c_\Omega = r d\theta/d\tau$ is the angular propagation speed. In the limit $L \gg 1$, the leading-order contribution to Eq. (3.35) is given by

$$\frac{1}{16} M_{\text{P}1}^4 r^8 f^2 L^2 (c_\Omega^2 - 1)^4 = 0. \quad (3.36)$$

This gives the following four solutions

$$c_\Omega^2 = 1. \quad (3.37)$$

From the above discussion, the four dynamical perturbations have the luminal speeds of propagation for high radial and angular momentum modes.

For $q_E \neq 0$ and $q_M = 0$, the perturbation Eqs. (3.27)-(3.30) separate into the two coupled equations for δA and χ_1 in the odd-parity sector and the other two coupled equations for χ_2 and v_1 in the even-parity sector. Since the isospectrality of QNMs between the odd- and even-parity modes holds in this case [51], we only need to integrate the two coupled differential equations in the odd-parity sector to compute the QNMs of purely electrically charged BHs.

For $q_M \neq 0$ and $q_E = 0$, the system described by Eqs. (3.27)-(3.30) separates into the following two types [62]: (I) χ_1 (odd-parity gravitational perturbation) and χ_2 (even-parity electromagnetic perturbation) are coupled with each other, and (II) δA (odd-parity electromagnetic perturbation) and v_1 (even-parity gravitational perturbation) are coupled with each other. In Ref. [63], it was shown that the isospectrality of QNMs between the types (I) and (II) holds for purely magnetically charged BHs. In this case, it is sufficient to calculate the QNMs for the perturbations of either type (I) or (II).

For $q_E \neq 0$ and $q_M \neq 0$, we observe in Eqs. (3.27)-(3.30) that the four dynamical perturbations δA , χ_1 , χ_2 , v_1 are coupled with each other. In such cases, we need to integrate the four coupled differential Eqs. (3.27)-(3.30) to compute the QNMs of BHs with mixed electric and magnetic charges.

IV. METHODS FOR COMPUTING QNMS

In this section, we will explain how to compute the QNMs of charged BHs given by the metric components (2.11). The perturbation equations of motion (3.27)-(3.30) can be expressed in the form

$$\left(\frac{d^2}{dt^2} - \frac{d^2}{dr_*^2}\right)\vec{\Psi} + \tilde{U}(r)\vec{\Psi}' + \tilde{V}(r)\vec{\Psi} = \vec{0}, \quad (4.1)$$

where $r_* = \int f^{-1} dr$ is the tortoise coordinate, $\vec{\Psi}$ is defined in Eq. (3.25), \tilde{U} and \tilde{V} are 4×4 matrices whose components depend on r and l .

For the BH solution (2.11), the horizons are located at the two radial distances r_+ and r_- satisfying

$$r^2 - 2Mr + \frac{q_E^2 + q_M^2}{2M_{\text{Pl}}^2} = (r - r_-)(r - r_+), \quad (4.2)$$

where $r_- < r_+$. Then, the tortoise coordinate can be expressed as

$$r_* = r + \frac{r_+^2}{r_+ - r_-} \ln\left(\frac{r - r_+}{r_+ + r_-}\right) - \frac{r_-^2}{r_+ - r_-} \ln\left(\frac{r - r_-}{r_+ + r_-}\right). \quad (4.3)$$

There are the following relations

$$2M = r_- + r_+, \quad \frac{q_E^2 + q_M^2}{2M_{\text{Pl}}^2} = r_- r_+. \quad (4.4)$$

For the later convenience, we introduce the dimensionless quantities

$$\alpha_E = \frac{q_E}{M_{\text{Pl}} r_+} = \sqrt{\frac{2r_-}{r_+}} \cos \alpha, \quad \alpha_M = \frac{q_M}{M_{\text{Pl}} r_+} = \sqrt{\frac{2r_-}{r_+}} \sin \alpha, \quad (4.5)$$

which satisfy the relation $\alpha_E^2 + \alpha_M^2 = 2r_-/r_+$.

We are interested in the propagation of perturbations in the region outside the external horizon, i.e., $r_+ < r < \infty$. For the computation of QNMs, it is convenient to introduce the new variables $\psi_1, \psi_2, \psi_3, \psi_4$ related to $v_1, \chi_1, \chi_2, \delta A$, respectively, as¹

$$v_1 = e^{-i\omega t} \frac{\psi_1}{M_{\text{Pl}}(r - r_+)}, \quad \chi_1 = e^{-i\omega t} \frac{\psi_2}{M_{\text{Pl}} r}, \quad \chi_2 = e^{-i\omega t} \frac{\psi_3}{r^2}, \quad \delta A = e^{-i\omega t} \psi_4. \quad (4.6)$$

Then, the perturbation Eqs. (4.1) reduce to the following form

$$\left[\frac{d^2}{dr_*^2} + \omega^2 - \mathbf{V}(r)\right]\vec{\psi} - \mathbf{U}(r)\vec{\psi}' = \vec{0}, \quad (4.7)$$

where \mathbf{U} and \mathbf{V} are 4×4 matrices depending on r and l , and

$$\vec{\psi} = (\psi_1, \psi_2, \psi_3, \psi_4)^T. \quad (4.8)$$

In the limit that $r \rightarrow r_+$, all the matrix components of $\mathbf{U}(r)$ and $\mathbf{V}(r)$ vanish. We also have the properties $\mathbf{U}(\infty) = \mathbf{0}$ and $\mathbf{V}(\infty) = \mathbf{0}$ at spatial infinity. This means that the perturbation Eqs. (4.7) reduce to

$$\left(\frac{d^2}{dr_*^2} + \omega^2\right)\psi_i = 0, \quad \text{for } r \rightarrow r_+ \text{ or } r \rightarrow \infty, \quad (4.9)$$

for each $i = 1, 2, 3, 4$. The solution to Eq. (4.9) can be expressed in the form $\psi_i = A_i e^{-i\omega r_*} + B_i e^{+i\omega r_*}$, where A_i and B_i are constants. Hence all the fields freely propagate around $r = r_+$ and $r \rightarrow \infty$. The QNMs correspond to the waves characterized by purely ingoing waves at the horizon and purely outgoing at spatial infinity, so that

$$\psi_i(r = r_+) = A_i e^{-i\omega r_*}, \quad \psi_i(r \rightarrow \infty) = B_i e^{+i\omega r_*}. \quad (4.10)$$

which are imposed as boundary conditions.

¹ To understand better the field redefinition for v_1 , let us reconsider all the metric perturbations and pick up the gauge-invariant combination $K_{\text{GI}} \equiv K - 2h h_1/r + h r G'$. In the gauge we have chosen, we have that $h_1 = -r h^{-1} K_{\text{GI}}/2$. Therefore around the horizon, $h_1 \propto K_{\text{GI}}/(r - r_+)$. To be more specific, the field v_1 , in our $K = 0 = G$ chosen gauge, really corresponds to the gauge-invariant combination $v_{1,\text{GI}} \equiv H_2 - L h_1/r + (r h' + L - 2h)/(2h) K - r K' + L r G'/2$, therefore around the horizon, up to a constant, $v_1 \simeq K/(r - r_+) + \dots$. Hence we have that $\psi_1 \simeq K_{\text{GI}}$, e.g., in the $h_1 = 0 = G$ gauge. It should be noted that the field K , at the horizon, becomes gauge invariant, so the field $\psi_1 \simeq K$ is a suitable variable to describe the behavior of perturbations close to it.

A. Expansion about the horizon

Now, we would like to find an approximate solution to the perturbation equations of motion around $r = r_+$. Since we have shown the asymptotic behavior of the fields ψ_i 's around the horizon, we will solve the perturbation equations order by order in the vicinity of $r = r_+$. For the computation of QNMs, we choose a purely ingoing wave expanded around $r = r_+$ in the form

$$\psi_i = e^{-i\omega r_*} \sum_{n=0}^{+\infty} \frac{G_i^{(n)}}{n!} (r - r_+)^n, \quad (4.11)$$

where $G_i^{(n)} = d^n G_i / dr^n|_{r=r_+}$ is the n -th derivative coefficient.

On using Eq. (4.3), the ingoing plane wave $e^{-i\omega r_*}$ in the vicinity of $r = r_+$ can be expressed as

$$e^{-i\omega r_*} = e^{-i\omega r} (r - r_+)^{-i\omega r_+^2 / (r_+ - r_-)} (r - r_-)^{i\omega r_-^2 / (r_+ - r_-)} \simeq C_1 (r - r_+)^{-i\omega r_+^2 / (r_+ - r_-)}, \quad (4.12)$$

where C_1 is a constant. Therefore, we look for an ansatz in terms of the radial variable r of the following type

$$\psi_i = (r - r_+)^b \sum_{n=0}^{+\infty} \frac{G_i^{(n)}}{n!} (r - r_+)^n, \quad \text{where} \quad b = -\frac{i\omega r_+^2}{r_+ - r_-}, \quad (4.13)$$

where we absorbed the constant C_1 into the definition of $G_i^{(n)}$.

We will solve Eqs. (4.7) order by order in $r - r_+$ to find constraints on the coefficients $G_i^{(n)}$. At lowest order, we can solve for the coefficients $G_i^{(1)}$ as functions of the coefficients $G_i^{(0)}$. At next order, we solve for $G_i^{(2)}$ as functions again of $G_i^{(0)}$. We repeat the iterations up to the required accuracy. It is clear that the dimension of the space of solutions is four, i.e., equal to the number of free parameters chosen for the coefficients $G_{1,2,3,4}^{(0)}$. For instance, we have

$$\begin{aligned} G_3^{(1)} = & -\frac{2\alpha_E L \alpha_M}{r_- + r_+ (2ir_+ \omega - 1)} G_4^{(0)} - \frac{2\alpha_E (r_- - r_+) (L - 2ir_+ \omega)}{[r_- - (L + 1)r_+] [r_- + r_+ (2ir_+ \omega - 1)]} G_1^{(0)} - \frac{L \alpha_M}{r_- + r_+ (2ir_+ \omega - 1)} G_2^{(0)} \\ & + \left[\frac{ir_-^2 \omega}{(r_- - r_+)^2} - i\omega - \frac{L}{r_- + r_+ (2ir_+ \omega - 1)} \right] G_3^{(0)}, \end{aligned} \quad (4.14)$$

where α_E and α_M are defined in Eq. (4.5).

B. Expansion at spatial infinity

Around spatial infinity, we also expand ψ_i 's corresponding to purely outgoing waves in the form

$$\psi_i = e^{i\omega r_*} \sum_{n=0}^{+\infty} \frac{F_i^{(n)}}{n!} r^{-n}, \quad (4.15)$$

where $F_i^{(n)} = d^n F_i / dr^n|_{r \rightarrow \infty}$. In this case, we have that

$$e^{i\omega r_*} = e^{i\omega r} \left(\frac{r - r_+}{r_+ + r_-} \right)^{i\omega r_+^2 / (r_+ - r_-)} \left(\frac{r - r_-}{r_+ + r_-} \right)^{-i\omega r_-^2 / (r_+ - r_-)} \simeq C_2 e^{i\omega r} r^{i\omega(r_+ + r_-)}, \quad (4.16)$$

where C_2 is a constant. Then, we can assume the solutions at spatial infinity, as

$$\psi_i = e^{kr} r^b \sum_{n=0}^{+\infty} \frac{F_i^{(n)}}{n!} r^{-n}, \quad k^2 = -\omega^2, \quad b = i\omega(r_+ + r_-) = -(r_+ + r_-) \frac{\omega^2}{k}, \quad (4.17)$$

where the QNMs correspond to $k = i\omega$. Note that we have absorbed the constant C_2 into the definition of $F_i^{(n)}$.

In the first iteration, the equations of motion can be solved for $F_i^{(1)}$ as functions of the four coefficients $F_i^{(0)}$. We can iterate the process leading to a recursive set of equations, which are used to express $F_i^{(n)}$ with $n \geq 2$ in terms of four $F_i^{(0)}$'s. Therefore, there are four free parameters at spatial infinity as well. For instance, we have

$$F_3^{(1)} = -\frac{2\alpha_E r_+}{L - 2} F_1^{(0)} + \frac{i [L - 2 (r_-^2 + r_+ r_- + r_+^2) \omega^2]}{2\omega} F_3^{(0)}. \quad (4.18)$$

If we use the expansion with higher values of n , we can compute the QNMs with higher accuracy.

C. Shooting from both the horizon and infinity

To compute the QNMs numerically, we will make use of the two methods explained below. These two choices are made for the purpose of confirming whether the different methods lead to the same results.

The first method is based on integrations of the coupled differential equations of four dynamical variables ψ_i ($i = 1, 2, 3, 4$) from the horizon toward larger r and from the spatial infinity toward smaller r . In doing so, we will exploit the series of solutions (4.13) and (4.17) expanded up to the thirteenth order. They automatically implement the necessary boundary conditions of QNMs. Since there are four independent choices of the coefficients $G_i^{(0)}$, we have a four-dimensional parameter space for the choices of initial conditions with respect to the integration from the horizon. There are also four independent choices of the boundary conditions associated with the coefficients $F_i^{(0)}$ for the inward integration from infinity.

Thus, we have four independent boundary conditions, respectively, both at the horizon and at spatial infinity. We call any of four independent solutions shooting from the horizon $\psi_i^{(h,j)}$. Here, the subscript i represents the dynamical perturbations, $j \in \{1, 2, 3, 4\}$ stands for the non-zero and equal-to-unity choice for $G_j^{(0)}$, and h indicates the solutions integrated from the horizon. For instance, if $j = 2$, then we have $G_2^{(0)} = 1$, whereas the other values of $G_j^{(0)}$ vanish. The integration of the perturbation equations of motion gives $\psi_i^{(h,j)}$ and $d\psi_i^{(h,j)}/dr$ at any radial distance. For the solutions $\psi_i^{(\infty,j)}$ integrated from infinity, we follow the same procedure by starting the integration at a sufficiently large distance (say, at $r = 100M$), where j represents the non-zero but equal-to-unity value for the coefficients $F_j^{(0)}$.

At this point, we can form an 8×8 matrix \mathcal{A} built as follows. Each of the first four columns, which is labeled by j , consists of the eight-dimensional column vector $[\psi_i^{(h,j)}, d\psi_i^{(h,j)}/dr]^T$. The remaining four columns are labeled again by j , but each of them is defined to be the eight-dimensional column vector $[\psi_i^{(\infty,j)}, d\psi_i^{(\infty,j)}/dr]^T$. We evaluate all the contributions forming the matrix \mathcal{A} at an intermediate matching point denoted by the distance r_{in} , say at $r = r_{\text{in}}$, where $r_+ < r_{\text{in}} < 100M$. If ω corresponds to the frequency of QNMs, these solutions are not linearly independent. This means that the determinant of \mathcal{A} vanishes, i.e.,

$$\det \mathcal{A} = 0, \quad (4.19)$$

at the matching radius r_{in} . If we correctly compute the QNM, it should be the same independent of the choice of r_{in} . This property can be used for the consistency check of numerical computations.

D. Shooting from the horizon to infinity

In this second method, we use the shooting integration method in a different way. Having the same solutions $\psi_i^{(h,j)}$ and $d\psi_i^{(h,j)}/dr$ as explained earlier, we evaluate them up to a sufficiently large distance, say, $r = r_{\text{max}} = 100M$. The resulting large-distance solutions do not generally satisfy the boundary conditions of QNMs, but they are the linear combinations of ingoing and outgoing waves. We set the onset of integration at $r = r_\epsilon \equiv r_+(1 + \epsilon)$ (with $\epsilon \simeq 10^{-3}$), as

$$\vec{\psi}|_{r=r_\epsilon} = \vec{\psi}_+ \left(G_i^{(0)}, r_\epsilon \right), \quad (4.20)$$

where $\vec{\psi}_+$ corresponds to the approximate solution whose components are given by Eq. (4.13). Then, we solve the perturbation equations of motion for each ψ_i up to the distance r_{max} . As mentioned above, the solutions for $\vec{\psi}|_{r=r_{\text{max}}}$ are in general the linear combinations of outgoing ($k = i\omega$) and ingoing ($k = -i\omega$) waves. It should be noted that the coefficients $F_i^{(j)}$ for $j > 0$ are linear functions of $F_i^{(0)}$, but they are generally functions of k as well. Since the QNMs correspond to $k = i\omega$, we name $F_i^{(0)}|_{k=i\omega} = F_i^{\text{QNM}}$. If we were to choose $k = -i\omega$, we would instead have ingoing waves corresponding to the quasi-bound states, for which $F_i^{(0)}|_{k=-i\omega} = F_i^{\text{QBS}}$. The solutions at $r = r_{\text{max}}$ can be generally expressed in the form

$$\psi_i|_{r=r_{\text{max}}} = B_{ij} F_j^{\text{QBS}} + C_{ij} F_j^{\text{QNM}}, \quad (4.21)$$

$$\psi'_i|_{r=r_{\text{max}}} = \tilde{B}_{ij} F_j^{\text{QBS}} + \tilde{C}_{ij} F_j^{\text{QNM}}, \quad (4.22)$$

where B_{ij} and C_{ij} characterize the coefficients of quasi-bound states and QNMs for $\psi_i|_{r=r_{\text{max}}}$, respectively (and the same applies to \tilde{B}_{ij} and \tilde{C}_{ij} for $\psi'_i|_{r=r_{\text{max}}}$). The left-hand sides of Eqs. (4.21) and (4.22) can be numerically found

by shooting from the horizon, whereas the right-hand sides are deduced by the Taylor-expanded solution given in Eq. (4.17) and its r derivative. Then, we can build up an 8×8 matrix \mathcal{M} with the elements defined as follows. We choose each of the first four columns of \mathcal{M} , which is labeled by j , to be the eight-dimensional column vector $[B_{ij}, \tilde{B}_{ij}]^T$ (for a fixed j). The remaining four columns are defined so that each of them, labeled now by $j + 4$, is the eight-dimensional column vector $[C_{ij}, \tilde{C}_{ij}]^T$ (for a fixed j). Then, we have a linear system given by

$$[\psi_i|_{r=r_\infty}, \psi'_i|_{r=r_\infty}]^T = \mathcal{M} [F_j^{\text{QBS}}, F_j^{\text{QNM}}]^T. \quad (4.23)$$

This equation can be solved for $[F_j^{\text{QBS}}, F_j^{\text{QNM}}]^T$. We repeat this procedure for each of the four independent boundary conditions around the horizon, labeled by a . Then, we can build a 4×4 matrix \mathcal{B} whose columns consist of the four solutions obtained for the F_j^{QBS} , or $\mathcal{B}_{ja} = F_j^{\text{QBS},a}$. The QNMs can be obtained by the condition that the determinant of \mathcal{B} vanishes, i.e.,

$$\det \mathcal{B} = 0. \quad (4.24)$$

For the system of coupled differential equations of four dynamical perturbations, this second method is numerically less efficient in comparison to the first method explained in Sec. IV C.

V. NUMERICAL DETERMINATION OF QNMS

In this section, we present the numerical results of the QNMs frequencies obtained by implementing the two methods explained in Sec. IV. We will show that, for a given total charge q_T and a BH mass M , the QNMs do not depend on the value of α , where we recall that $\tan \alpha = q_M/q_E$. In other words, we see the isospectrality for the quasinormal frequency, i.e., the degeneracy of ω 's in terms of the parameter α . We deduce this isospectrality by using a numerical approach. As such, we will prove it for a finite number of the parameters of solutions. We mainly study the two fundamental mode frequencies (gravitational and electromagnetic) for $l = 2$ by fixing the BH mass, but changing the value of q_T in the range $0 < q_T^2 < 2M_{\text{P1}}^2 r_+^2$ (the upper bound evaluated in the extremal case, for which $r_+ = r_- = M$). We show that, for the method explained in Sec. IV, the solutions satisfy $\det \mathcal{A} = 0$ also when evaluated on different values of α , i.e., changing the value of q_E/q_M (while keeping the same value of $q_T^2 = q_E^2 + q_M^2$). We also briefly discuss the $l = 3$ gravitational fundamental tone as well as one single example of the overtones. In all these cases, we report that the quasinormal frequencies of the considered modes do not depend on α .

In the following, we fix units for which the BH mass is $M = 1$, so that $r_+ + r_- = 2$. We also assume that $0 \leq r_- \leq r_+$, in which case $0 \leq r_- \leq M$. In the limit $r_- \rightarrow 0$, we have $q_T^2 = 2M_{\text{P1}}^2 r_- r_+ \rightarrow 0$ and $r_+ \rightarrow 2$, independently of the value of α . In this limit, the spectrum of QNMs tends to coincide with the one of an uncharged Schwarzschild BH solution [44–46]. Instead, as already mentioned, the extremal charged BH corresponds to $r_- = r_+ \rightarrow M$.

Without the loss of generality, we will consider the BHs with positive electric and (or) magnetic charges. For the purely electrically charged BH, we have $\alpha = 0$, whereas the purely magnetic BH corresponds to $\alpha = \pi/2$. The BHs with mixed electric and magnetic charges have the angle $0 < \alpha < \pi/2$. For a fixed value of r_- , the external horizon $r_+ = 2 - r_-$ is determined accordingly. This fixes the background metric components as $f = h = (r - r_-)(r - r_+)/r^2$, with the squared total charge $q_T^2 = 2M_{\text{P1}}^2 r_- r_+$. For a given q_T , there are infinite possibilities for q_M to give the same total charge. In particular, we have chosen to parameterize these possibilities by introducing the parameter α such that $q_E = M_{\text{P1}} \sqrt{2r_- r_+} \cos \alpha$ and $q_M = M_{\text{P1}} \sqrt{2r_- r_+} \sin \alpha$. While the BH solutions with different values of α are not distinguished in the metric field profile at the background level, the perturbation equations presented in Sec. III do have the dependence on α . As such, we are tempted to think that the QNMs may also depend on the value of α , i.e., being able to discriminate a magnetic BH from an electric one. However, the numerical results presented here will show that this is not the case.

To compute the QNMs numerically with a given value of α , we solve the discriminant Eqs. (4.19) or (4.24) for each r_- , by using the QNM obtained for the previous value of r_- as an initial guess for ω . We perform the integration procedure by starting from small values of r_- close to 0. In the limit $r_- \rightarrow 0$, the QNM in the gravitational sector should agree with the one for the Schwarzschild BH. For each value of r_- , the discriminant equations are solved with an error at most of order 10^{-7} . As we mentioned before, we will mostly exploit the first method explained in Sec. IV C due to its efficiency, but we will also carry out the integration with the second method given in Sec. IV D to confirm the consistency of our numerical results.

In Fig. 1, we plot the numerical values of the quasinormal frequency $\omega = \omega_R + i\omega_I$ of the gravitational fundamental mode with $l = 2$ for $\alpha = 0$, where the left and right panels represent the real and imaginary parts of ωM versus r_-/M . In Fig. 2, we show the electromagnetic fundamental modes for $l = 2$, which are called “electro-quadrupole” quasinormal frequencies [58]. We can repeat the same procedure explained above for any value of q_T^2 by changing

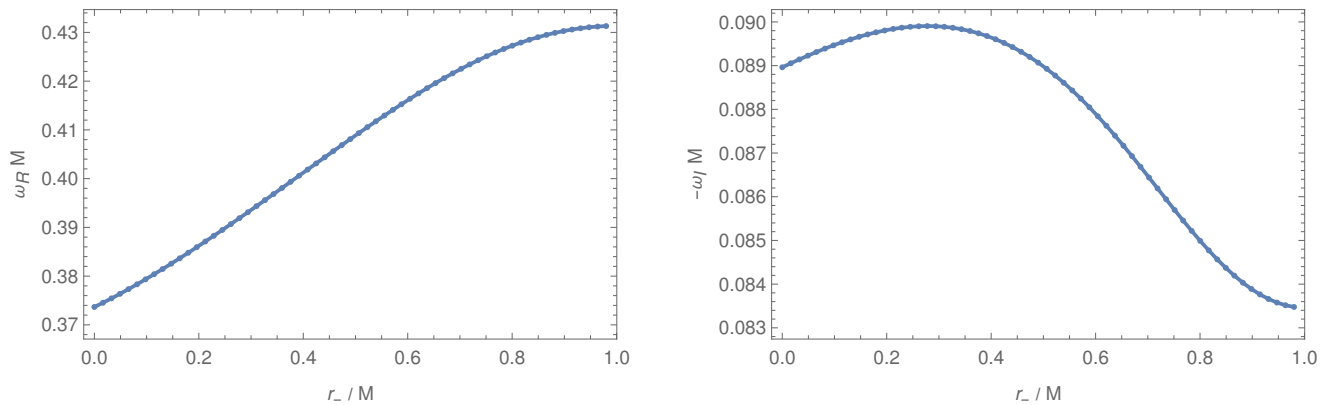


FIG. 1. The QNMs for the $l = 2$ gravitational fundamental mode in the purely electric case, i.e., $\alpha = 0$. The left and right panels show the real and imaginary parts of QNMs as a function of r_- , which is in the range $0 \leq r_- \leq M$. In the limit $r_- \rightarrow 0$, the gravitational QNM approaches the one in the Schwarzschild case: $\omega M = 0.37367 - 0.08896i$. The extremal charged BH corresponds to the limit $r_- \rightarrow M$.

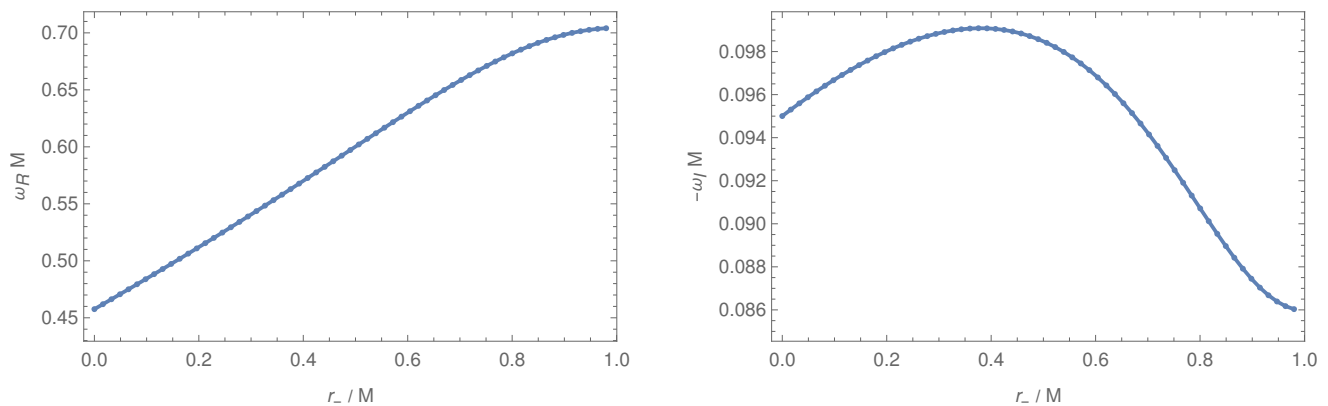


FIG. 2. The QNMs for the $l = 2$ electromagnetic fundamental mode in the purely electric case ($\alpha = 0$). The meanings of the left and right panels are the same as those in Fig. 1. In the limit $r_- \rightarrow 0$, the electromagnetic QNM approaches the value $\omega M = 0.45760 - 0.09500i$.

the ratio q_M/q_E , i.e., changing the value of α . In this case, we find that the resulting quasinormal frequencies are numerically indistinguishable from those obtained for $\alpha = 0$. This means that the QNMs are independent of α . When $\alpha = 0$, the QNMs correspond to those for the purely electrically charged BH solution, in which case the perturbation Eqs. (3.27)-(3.30) separate into those in the odd- and even-parity sectors. When $q_M = 0$, the isospectrality is known to hold between odd- and even-parity perturbations [51–53, 58] and hence we only need to compute the QNMs in the odd-parity sector arising from the gravitational field χ_1 and the electromagnetic field δA . When $q_M \neq 0$ and $q_E = 0$, the even modes couple to the odd ones, but the perturbation equations separate into the types (I) and (II) to give the same QNM spectra between the two types [63].

As already stated above, for small values of r_- close to 0, the gravitational QNMs tend to approach those of the Schwarzschild BH. Indeed, for the case $l = 2$, $r_- = 10^{-6}$ and $\alpha = 10^{-6}$, we numerically obtain the value $\omega M = 0.37367 - 0.08896i$, which is in agreement with the value of the uncharged, non-rotating BH in GR [44–46]. In the same $r_- \rightarrow 0$ limit, the electromagnetic QNM approaches the value $\omega M = 0.45760 - 0.09500i$ known for a decoupling limit of the electromagnetic field from gravity in the $l = 2$ case [53]. For all values of r_- between 0 and M , we confirm that the gravitational and electromagnetic QNMs are in good agreement with those derived in Ref. [53].

Hence, up to this point, our results of QNMs match with those obtained for the electrically charged BH known in the literature. In the following, we will present new results for the BHs with magnetic and electric charges. In Fig. 3, we show the differences $[\omega(\alpha) - \omega(\alpha = \pi/4)]M$ for several different values of α ($\alpha = 0, \pi/3, \pi/2$) in comparison to the $\alpha = \pi/4$ case. Since very tiny differences of order 10^{-11} are merely induced by the truncation of solutions at two

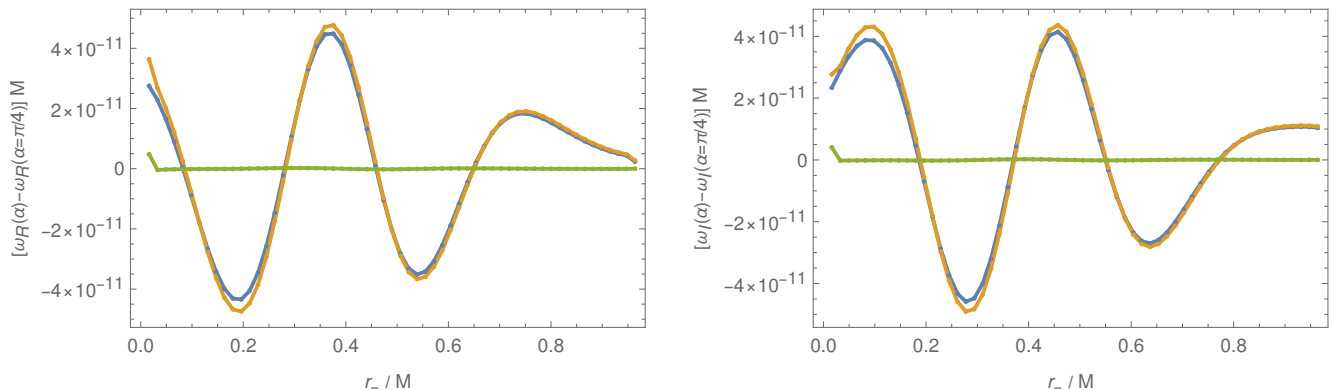


FIG. 3. Differences of the QNMs for several values of α compared to the equally mixed charged BH ($\alpha = \pi/4$, or $q_E = q_M$). The left and right panels correspond to the differences of the real and imaginary parts of fundamental QNMs with $l = 2$, respectively. The blue and orange lines refer to the purely magnetic BH ($\alpha = \pi/2$, or $q_E = 0$) and the purely electric BH ($\alpha = 0$, or $q_M = 0$), whereas the green line corresponds to the case $\alpha = \pi/3$. For a given value of r_- , we have $q_T^2 = 2M_{\text{Pl}}^2 r_- r_+$ with $r_+ = 2 - r_-$ and $0 \leq r_- \leq 1$ in the unit $M = 1$, so that increasing r_- means to increase the value of q_T .

boundaries, we deduce that the fundamental QNMs with $l = 2$ are independent of α . In other words, for any values of α , the quantity $[\omega(\alpha) - \omega(\alpha = \pi/4)]M$ is consistent with 0 up to the numerical precision we had to determine the values of ω themselves.

Another way to show the isospectrality of QNMs is to evaluate the solutions found for a fixed value of α and verify that the discriminant equation $\det \mathcal{A} = 0$ is well satisfied (up to numerical errors) independently of the value of α . We recall that \mathcal{A} is the 8×8 matrix derived by the shooting from both the horizon and spatial infinity. Up to the numerical precision of order 10^{-7} , the determinant of \mathcal{A} does not depend on α for any given total charge q_T (i.e., for fixed r_-). We also confirm that different choices for the matching distance r_{in} do not affect the value of the quasinormal frequencies. The second integration method based on the determinant of \mathcal{B} also gives rise to the same values of QNMs and their independence on α .

So far we have dealt with the fundamental modes for $l = 2$. In the following, we investigate other quasinormal frequencies and show their independence on the value of α . In Fig. 4, we plot the QNMs of purely electrically charged BHs ($\alpha = 0$) for the $l = 3$ fundamental gravitational mode versus r_-/M . In the limit $r_- \rightarrow 0$, the gravitational QNM approaches the value $\omega M = 0.59944 - 0.09270i$, which coincides with the one obtained for the Schwarzschild BH. The qualitative behavior of the real and imaginary parts of ω concerning the change of r_- is similar to that for the case $l = 2$. For $\alpha \neq 0$, we find that the QNMs for the $l = 3$ gravitational fundamental mode with given q_T and M are the same as those derived for $\alpha = 0$ up to the numerical precision of order 10^{-7} . Indeed, this property can be confirmed by the computation of $\det \mathcal{A}$ for several different values of α . We also computed the $l = 3$ fundamental electromagnetic QNMs and found that, for fixed q_T and M , they are independent of α .

Finally, we also study the QNM of one single overtone. To search for the overtones, we need to further increase the numerical precision of integration of the differential equations, leading evidently to a longer time to solve the discriminant equation. For $l = 2$ and $r_- = 2/5$, we obtain the overtone frequency $\omega M \simeq 0.507 - 0.234i$. For this solution, the two shooting methods explained in Sec. IV C and IV D give good convergence to the same QNM. Once we get this convergence, we again see the independence on α of the discriminant equation up to the order of 8×10^{-5} .

This shows that, at least up to the numerical precision we have reached, we cannot discriminate the purely magnetic (or electromagnetic) BHs from the purely electric BHs. In other words, the model parameters on which the QNMs depend are the BH mass and the squared total charge $q_T^2 = q_E^2 + q_M^2$ alone. As a consequence, at least regarding the quasinormal frequencies, the most general static electromagnetic BHs do not acquire a new hair associated with the extra parameter α .

This conclusion is far from obvious. If we consider the pseudo-scalar invariant $F_{\mu\nu} \tilde{F}^{\mu\nu}$, which corresponds to the inner product of the electric and magnetic fields, we have $|F_{\mu\nu} \tilde{F}^{\mu\nu}| = 4|q_E q_B|/r^4$, for which both the electric and magnetic fields are radial in the BH rest frame. Therefore, the purely electric case ($\alpha = 0$) or the purely magnetic case ($\alpha = \pi/2$) would make the invariant vanish at the background level. For α in the range $0 < \alpha < \pi/2$, say for $\alpha = \pi/4$ (i.e., $q_E = q_M$), this invariant does not vanish any longer. Hence, we could at least in principle expect intrinsically different properties for the BHs with mixed electric and magnetic charges. With a given total charge q_T and mass M , however, we have shown that the QNMs for fixed l are the same independently of the mixing between the electric and

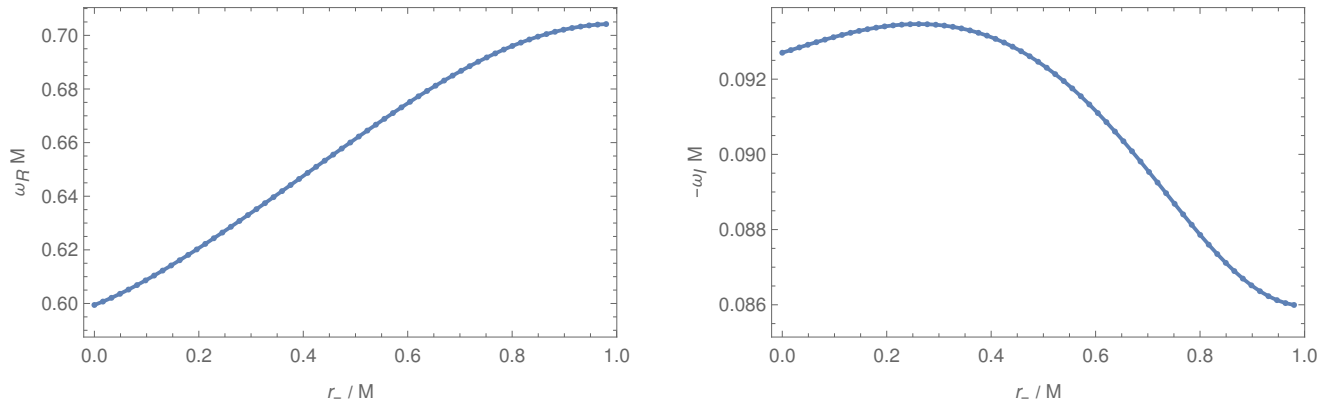


FIG. 4. The QNMs for the $l = 3$ gravitational fundamental mode. Although the numerical calculations have been performed for $\alpha = 0$, the corresponding QNMs for $\alpha \neq 0$ are the same up to numerical errors.

magnetic charges. In other words, if the gravitational wave observations were to measure the same QNMs predicted by the electrically charged RN BH, there are also possibilities that the BH has a pure magnetic charge or a mixture of magnetic and electric charges.

VI. CONCLUSIONS

In this paper, we studied the quasinormal frequencies of SSS BHs carrying both electric and magnetic charges. The QNMs of an electrically charged BH were computed in the 1980's by using the BH perturbation theory. In this case, the perturbation equations of motion can be decomposed into odd- and even-parity modes, each of which contains two dynamical degrees of freedom in the gravitational and electromagnetic sectors. Due to the isospectrality of purely electrically charged BHs in GR, the QNMs are the same for both odd- and even-parity perturbations.

For purely magnetically charged BHs, there are two types of dynamical perturbations which can be separated into two coupled differential equations [62], i.e., (I) odd-parity gravitational perturbation χ_1 and even-parity electromagnetic perturbation χ_2 are coupled with each other, and (II) odd-parity electromagnetic perturbation δA and even-parity gravitational perturbation v_1 are coupled with each other. In this case, the isospectrality of QNMs holds between the types (I) and (II) [63]. Hence the two QNMs corresponding to the gravitational and electromagnetic degrees of freedom can be computed by using the perturbation equations in type (I) or (II).

For BHs with mixed electric and magnetic charges, we derived the perturbation equations of motion in Eqs. (3.27)-(3.30) for the dynamical degrees of freedom δA , χ_1 , χ_2 , and v_1 . Provided that $q_E \neq 0$ and $q_M \neq 0$, the four dynamical perturbations are coupled with each other. For high radial and angular momentum modes, we showed that the no-ghost conditions are trivially satisfied outside the external horizon, with the luminal propagation speeds of dynamical perturbations in both radial and angular directions. The mixing between the magnetic and electric charges is weighed by a parameter α . The main point of this paper is to elucidate whether the charged BH has an extra hair associated with the parameter α , besides the BH mass M and the total charge q_T .

We showed that, for a given total charge q_T and mass M , the fundamental QNMs with a fixed multipole l do not depend on the mixing angle α . In Figs. 1 and 2, we plotted the fundamental quasinormal frequencies of gravitational and electromagnetic perturbations for $l = 2$ and $M = 1$. Depending on the value of r_- (or on the total charge q_T), the real and imaginary parts of QNMs are different and hence they can be distinguished from those of the uncharged Schwarzschild solution. However, as we see e.g., in Fig. 3, both the gravitational and electromagnetic QNMs are independent of α up to the numerical precision of order 10^{-11} . We also studied the overtones and confirmed the similar independence on α .

The above results show that the electric and magnetic BHs cannot be distinguished from each other by using the observations of QNMs alone. In other words, the observational identification of QNMs being the same as those theoretically predicted by the RN BH does not imply that the BH is purely electrically charged. It can be magnetically charged or in a mixed state with magnetic and electric charges. However, the dynamics of charged (standard) particles in the vicinity of BHs are different between the electrically and magnetically charged BHs. Hence there should be some other ways of distinguishing between the two cases. It will be of interest to see whether future observations can find some signatures of magnetically charged BHs.

ACKNOWLEDGEMENTS

We thank Nicolas Yunes for useful discussions about the QNMs of BHs and isospectrality. The work of ADF was supported by the Japan Society for the Promotion of Science Grants-in-Aid for Scientific Research No. 20K03969. ST is supported by the Grant-in-Aid for Scientific Research Fund of the JSPS No. 22K03642 and Waseda University Special Research Project No. 2023C-473.

-
- [1] A. Einstein, *Annalen Phys.* **49**, 769 (1916).
 [2] K. Schwarzschild, *Sitzungsber. Preuss. Akad. Wiss. Berlin (Math. Phys.)* **1916**, 189 (1916), arXiv:physics/9905030.
 [3] H. Reissner, *Annalen Phys.* **355**, 106 (1916).
 [4] G. Nordstrom, *Phys. Z.* **15**, 504 (1914), arXiv:physics/0702221.
 [5] J. Maldacena, *JHEP* **04**, 079 (2021), arXiv:2004.06084 [hep-th].
 [6] Y. Bai and M. Korwar, *JHEP* **04**, 119 (2021), arXiv:2012.15430 [hep-ph].
 [7] D. Stojkovic and K. Freese, *Phys. Lett. B* **606**, 251 (2005), arXiv:hep-ph/0403248.
 [8] T. Kobayashi, *Phys. Rev. D* **104**, 043501 (2021), arXiv:2105.12776 [hep-ph].
 [9] S. Das and A. Hook, *JHEP* **12**, 145 (2021), arXiv:2109.00039 [hep-ph].
 [10] J. Estes, M. Kavic, S. L. Liebling, M. Lippert, and J. H. Simonetti, *JCAP* **06**, 017 (2023), arXiv:2209.06060 [astro-ph.HE].
 [11] C. Zhang and X. Zhang, *JHEP* **10**, 037 (2023), arXiv:2302.07002 [hep-ph].
 [12] Y. Bai, J. Berger, M. Korwar, and N. Orlofsky, *JHEP* **10**, 210 (2020), arXiv:2007.03703 [hep-ph].
 [13] D. Ghosh, A. Thalappilil, and F. Ullah, *Phys. Rev. D* **103**, 023006 (2021), arXiv:2009.03363 [hep-ph].
 [14] K. Akiyama *et al.* (Event Horizon Telescope), *Astrophys. J. Lett.* **875**, L1 (2019), arXiv:1906.11238 [astro-ph.GA].
 [15] P. Kocherlakota *et al.* (Event Horizon Telescope), *Phys. Rev. D* **103**, 104047 (2021), arXiv:2105.09343 [gr-qc].
 [16] G. W. Gibbons and K.-i. Maeda, *Nucl. Phys. B* **298**, 741 (1988).
 [17] D. Garfinkle, G. T. Horowitz, and A. Strominger, *Phys. Rev. D* **43**, 3140 (1991), [Erratum: Phys.Rev.D 45, 3888 (1992)].
 [18] R. Kallosh, A. D. Linde, T. Ortin, A. W. Peet, and A. Van Proeyen, *Phys. Rev. D* **46**, 5278 (1992), arXiv:hep-th/9205027.
 [19] A. Sen, *Phys. Rev. Lett.* **69**, 1006 (1992), arXiv:hep-th/9204046.
 [20] L. Liu, O. Christiansen, Z.-K. Guo, R.-G. Cai, and S. P. Kim, *Phys. Rev. D* **102**, 103520 (2020), arXiv:2008.02326 [gr-qc].
 [21] L. Liu, O. Christiansen, W.-H. Ruan, Z.-K. Guo, R.-G. Cai, and S. P. Kim, *Eur. Phys. J. C* **81**, 1048 (2021), arXiv:2011.13586 [gr-qc].
 [22] Z.-C. Chen, S. P. Kim, and L. Liu, *Commun. Theor. Phys.* **75**, 065401 (2023), arXiv:2210.15564 [gr-qc].
 [23] H.-T. Wang, P.-C. Li, J.-L. Jiang, G.-W. Yuan, Y.-M. Hu, and Y.-Z. Fan, *Eur. Phys. J. C* **81**, 769 (2021), arXiv:2004.12421 [gr-qc].
 [24] V. Cardoso, C. F. B. Macedo, P. Pani, and V. Ferrari, *JCAP* **05**, 054 (2016), [Erratum: JCAP 04, E01 (2020)], arXiv:1604.07845 [hep-ph].
 [25] O. Christiansen, J. Beltrán Jiménez, and D. F. Mota, *Class. Quant. Grav.* **38**, 075017 (2021), arXiv:2003.11452 [gr-qc].
 [26] N. Yunes and F. Pretorius, *Phys. Rev. D* **80**, 122003 (2009), arXiv:0909.3328 [gr-qc].
 [27] J. Alsing, E. Berti, C. M. Will, and H. Zaglauer, *Phys. Rev. D* **85**, 064041 (2012), arXiv:1112.4903 [gr-qc].
 [28] N. Yunes, P. Pani, and V. Cardoso, *Phys. Rev. D* **85**, 102003 (2012), arXiv:1112.3351 [gr-qc].
 [29] T. Liu, W. Zhao, and Y. Wang, *Phys. Rev. D* **102**, 124035 (2020), arXiv:2007.10068 [gr-qc].
 [30] Y. Higashino and S. Tsujikawa, *Phys. Rev. D* **107**, 044003 (2023), arXiv:2209.13749 [gr-qc].
 [31] H.-Y. Yuan, H.-J. Lü, J. Rice, and E.-W. Liang, *Phys. Rev. D* **108**, 083018 (2023), arXiv:2309.13840 [astro-ph.HE].
 [32] B. Zhang, *Astrophys. J. Lett.* **873**, L9 (2019), arXiv:1901.11177 [astro-ph.HE].
 [33] R. Niu, X. Zhang, B. Wang, and W. Zhao, *Astrophys. J.* **921**, 149 (2021), arXiv:2105.13644 [gr-qc].
 [34] H. Takeda, S. Tsujikawa, and A. Nishizawa, arXiv:2311.09281 [gr-qc].
 [35] M. Quartin, S. Tsujikawa, L. Amendola, and R. Sturani, *JCAP* **08**, 049 (2023), arXiv:2304.02535 [astro-ph.CO].
 [36] K. D. Kokkotas and B. G. Schmidt, *Living Rev. Rel.* **2**, 2 (1999), arXiv:gr-qc/9909058.
 [37] H.-P. Nollert, *Class. Quant. Grav.* **16**, R159 (1999).
 [38] E. Berti, V. Cardoso, and A. O. Starinets, *Class. Quant. Grav.* **26**, 163001 (2009), arXiv:0905.2975 [gr-qc].
 [39] R. A. Konoplya and A. Zhidenko, *Rev. Mod. Phys.* **83**, 793 (2011), arXiv:1102.4014 [gr-qc].
 [40] P. Pani, *Int. J. Mod. Phys. A* **28**, 1340018 (2013), arXiv:1305.6759 [gr-qc].
 [41] T. Regge and J. A. Wheeler, *Phys. Rev.* **108**, 1063 (1957).
 [42] F. J. Zerilli, *Phys. Rev. Lett.* **24**, 737 (1970).
 [43] F. J. Zerilli, *Phys. Rev. D* **2**, 2141 (1970).
 [44] S. Chandrasekhar and S. L. Detweiler, *Proc. Roy. Soc. Lond. A* **344**, 441 (1975).
 [45] S. Chandrasekhar, *Proc. Roy. Soc. Lond. A* **343**, 289 (1975).
 [46] S. Chandrasekhar, *The mathematical theory of black holes* (1985).
 [47] V. Moncrief, *Phys. Rev. D* **9**, 2707 (1974).
 [48] V. Moncrief, *Phys. Rev. D* **10**, 1057 (1974).
 [49] V. Moncrief, *Phys. Rev. D* **12**, 1526 (1975).
 [50] F. J. Zerilli, *Phys. Rev. D* **9**, 860 (1974).

- [51] S. Chandrasekhar, *Proc. Roy. Soc. Lond. A* **369**, 425 (1980).
- [52] D. L. Gunter, *Phil. Trans. Roy. Soc. Lond* **A296**, 497 (1980).
- [53] K. D. Kokkotas and B. F. Schutz, *Phys. Rev. D* **37**, 3378 (1988).
- [54] B. F. Schutz and C. M. Will, *Astrophys. J. Lett.* **291**, L33 (1985).
- [55] S. Iyer and C. M. Will, *Phys. Rev. D* **35**, 3621 (1987).
- [56] E. W. Leaver, *Proc. Roy. Soc. Lond. A* **402**, 285 (1985).
- [57] E. W. Leaver, *Phys. Rev. D* **34**, 384 (1986).
- [58] E. W. Leaver, *Phys. Rev. D* **41**, 2986 (1990).
- [59] E. Berti and K. D. Kokkotas, *Phys. Rev. D* **68**, 044027 (2003), arXiv:hep-th/0303029.
- [60] H. Onozawa, T. Mishima, T. Okamura, and H. Ishihara, *Phys. Rev. D* **53**, 7033 (1996), arXiv:gr-qc/9603021.
- [61] N. Andersson and H. Onozawa, *Phys. Rev. D* **54**, 7470 (1996), arXiv:gr-qc/9607054.
- [62] K. Nomura, D. Yoshida, and J. Soda, *Phys. Rev. D* **101**, 124026 (2020), arXiv:2004.07560 [gr-qc].
- [63] K. Nomura and D. Yoshida, *Phys. Rev. D* **105**, 044006 (2022), arXiv:2111.06273 [gr-qc].
- [64] R. Kase and S. Tsujikawa, *Phys. Rev. D* **107**, 104045 (2023), arXiv:2301.10362 [gr-qc].